Structurally Modulated Magnetic Properties in the $A_3MnRu_2O_9$ Phases (A = Ba, Ca): The Role of Metal−Metal Bonding in Perovskite-Related Oxides

Z. Serpil Gönen,[1a] J. Gopalakrishnan,[1a,b,c] B. W. Eichhorn,[1a] and Richard L. Greene[1c]

Center for Superconductivity Research, Department of Physics and Department of Chemistry and Biochemistry, University of Maryland, College Park, Maryland 20742

Received November 28, 2000

$Ca_3MnRu_2O_9$ and $Ba_3MnRu_2O_9$ were synthesized from transition metal dioxides and alkaline earth metal carbonates at 1100−1300 °C. $Ca_3MnRu_2O_9$ adopts the prototypical $GdFeO_3$-type perovskite structure with Mn and Ru statistically disordered over the single metal atom site. The susceptibility shows Curie−Weiss behavior above 240 K with $\mu_{eff} = 3.14\ \mu_B$/metal atom, which is in excellent agreement with the expected spin-only moment of 3.20 μ_B. Below 150 K, the compound shows spin-glass-like short-range ferrimagnetic correlations. The high-temperature region of the electrical resistivity reveals a small activation energy of 17(1) meV whereas the low-temperature region is nonlinear and does not fit a variable range hopping model. $Ba_3MnRu_2O_9$ crystallizes in the 9-layer $BaRuO_3$-type structure containing M_3O_{12} face-shared trioctahedral clusters in which Mn and Ru are statistically disordered. $Ba_3MnRu_2O_9$ shows nonlinear reciprocal susceptibility at all temperatures and is described by a variable-spin cluster model with an $S = {}^1/_2$ ground state with thermally populated excited states. The low spin value of this system ($S = {}^1/_2$) is attributed to direct metal−metal bonding. Below 30 K, the compound shows short-range magnetic correlations and spin-glass-like behavior. The high-temperature region of the electrical resistivity indicates a small activation energy of 8.8(1) meV whereas the low-temperature region is nonlinear. The importance of metal−metal bonding and the relationships to other related compounds are discussed.

Introduction

The compounds $BaTiO_3$ and $BaNiO_3$ represent structural end members of the ABO_3 perovskite-related oxides.[2,3] One form of $BaTiO_3$ is that of the ideal cubic perovskite (space group $Pm\bar{3}m$) defined by a three-dimensional structure built of corner-shared TiO_6 octahedra. Several distortions from ideal cubic symmetry are known including the common $GdFeO_3$ structure that has undistorted MO_6 octahedra linked in a buckled fashion (**I**).[4] In contrast, $BaNiO_3$ adopts a pseudo-one-dimensional structure (space group $P6_3/mmc$) with face-shared NiO_6 chains extending along the *c* axis of the hexagonal cell (**II**). In the $BaNiO_3$ structure, there are short metal−metal contacts along the chains (∼2.5−2.9 Å) that can affect the magnetic and transport properties of the compounds. Several different polytypes are known that can be described as intergrowths of these two end members. For example, the 6-layer (6H) and 9-layer (9R) structures are composites of the two end members and contain both corner- and face-shared octahedra (see **III** and **IV**). In the 6H structure, there are face-shared bioctahedral units (FSBOs) separated by layers of corner-shared octahedra. In the 9R structure, there are face-shared trioctahedral units (FSTOs) that are linked by shared corners. Although the structural motifs have been well established for the various polytypes and many of the properties characterized, a systematic analysis of the effects of direct metal−metal bonding in the FSBOs and FSTOs has yet to be established.

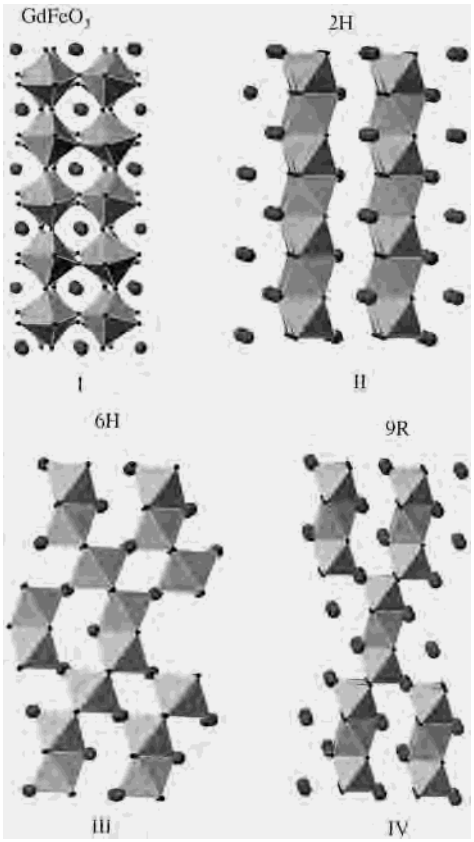

In contrast to the solid state oxides, the ternary halides containing FSBO units have been well studied.[5] In addition, the molecular analogues of these ternary halides (and their derivatives) have been prepared and their properties are now

(1) (a) Maryland, Chemistry. (b) On leave from Indian Institute of Science, Bangalore. (c) Maryland, Physics.
(2) Rao, C. N. R.; Gopalakrishnan, J. *New Directions in Solid State Chemistry*, 2nd ed.; Cambridge University Press: Cambridge, U.K., 1997.
(3) Wells, A. F. *Structural Inorganic Chemistry*, 5th ed.; Oxford University Press: New York, 1984.
(4) Geller, S. *J. Chem. Phys.* **1956**, *24*, 1236.

10.1021/ic0013431 CCC: $20.00
Published on Web 08/15/2001

well understood. Perhaps the most well-known of these systems, the $A_3M_2X_9$ phases (A = alkali; M = Cr, Mo, W, Ru; X = halide),[6−11] have variable ground states that are both metal and halide dependent. For example, the tungsten phases have $S = 0$, diamagnetic ground states with tungsten−tungsten triple bonds[12,13] whereas the Cr compounds are paramagnetic with $S = {}^3/_2$ ground states in which the Cr^{3+} ions show only weak antiferromagnetic coupling.[6,8,9,14,15] The Mo systems are intermediate to these cases having diamagnetic ground states with thermally populated paramagnetic excited states that give rise to temperature dependent spin systems.[10,11] The degree of M−M bonding is directly correlated to the magnetic behavior and can be analyzed in terms of the Cotton−Ucko criterion.[16] Molecular FSBO and FSTO systems are also well-known and can be described in a similar manner.[16−19]

Recently, Felser, Rijssenbeek, and co-workers have characterized the magnetic properties of $BaRuO_3$ in terms of metal−metal bonding that affect the overall transport properties of these compounds.[20,21] The 4-layer (4H) and 9-layer (9R) forms of $BaRuO_3$ contain FSBO and FSTO units, respectively. In previous studies, it was shown that substitution of $^1/_3$ of the Ru sites in $BaRuO_3$ gives $Ba_3MRu_2O_9$ phases where M = Fe, Co, Ni, Cu, In.[22] These compounds adopt the 6-layer 6H structure containing FSBOs separated by corner-shared octahedra (see **III**). With the exception of the iron phase, the Ru atoms were completely localized in the FSBOs with the M atoms residing in the corner-shared octahedra. Rijssenbeck et al. recently showed that the transport and magnetic properties could be understood on the basis of this ordered model.[22] Interestingly, Mn substitution in 9R $BaRuO_3$ was previously described by Donohue et al.[23] to give the M = Mn member of this series, $Ba_3MnRu_2O_9$. Although they observed a spontaneous decrease in the cell parameters with the increase in Mn content, the structural details and physical properties were not described. Herein, we report the synthesis and characterization of two isoelectronic manganese ruthenates, $Ba_3MnRu_2O_9$ and $Ca_3MnRu_2O_9$. Unlike the other $Ba_3MRu_2O_9$ phases,[22] $Ba_3MnRu_2O_9$ adopts the 9-layer 9R structure (**IV**) and is described by a variable-spin FSTO model. In contrast, $Ca_3MnRu_2O_9$ adopts the $GdFeO_3$ distorted perovskite structure (**I**) and shows Curie−Weiss behavior. The analysis of the direct metal−metal interactions and comparisons with other oxides and related halides are discussed.

(5) Cotton, F. A.; Walton, R. A. *Multiple Bonds Between Metal Atoms*, 2nd ed.; Oxford University Press: New York, 1993.
(6) Ajiro, Y.; Kikuchi, H.; Inami, T.; Sakakibara, T.; Goto, T. *J. Phys. Soc. Jpn.* **1989**, *58*, 1021.
(7) Grey, I. E.; Smith, P. W. *Aust. J. Chem.* **1971**, *24*, 73.
(8) Leuenberger, B.; Güdel, H. U.; Fischer, P. *J. Solid State Chem.* **1986**, *64*, 90.
(9) Saillant, R.; Jackson, R. B.; Streib, W. E.; Folting, K.; Wentworth, R. A. D. *Inorg. Chem.* **1971**, *10*, 1453.
(10) Stranger, R.; Grey, I. E.; Madsen, I. C.; Smith, P. W. *J. Solid State Chem.* **1987**, *69*, 162.
(11) Stranger, R.; Smith, P. W.; Grey, I. E. *Inorg. Chem.* **1989**, *28*, 1271.
(12) Dunbar, K. R.; Pence, L. E. *Acta Crystallogr.* **1990**, *C47*, 23.
(13) Watson, W. H.; Waser, J. *Acta Crystallogr.* **1958**, *11*, 689.
(14) Kahn, O.; Briat, B. *Chem. Phys. Lett.* **1975**, *32*, 376.
(15) Wessel, G. J.; Ijdo, D. J. W. *Acta Crystallogr.* **1957**, *10*, 466.
(16) Cotton, F. A.; Ucko, D. A. *Inorg. Chim. Acta* **1972**, *6*, 161.
(17) Fettinger, J. C.; Gordon, J. C.; Mattamana, S. P.; O'Connor, C. J.; Poli, R.; Salem, G. *Inorg. Chem.* **1996**, *35*, 7404.
(18) Bino, A.; Cotton, F. A. *J. Am. Chem. Soc.* **1980**, *102*, 608.
(19) Bursten, B. E.; Cotton, F. A.; Fang, A. *Inorg. Chem.* **1983**, *22*, 2127.
(20) Felser, C.; Cava, R. J. *Phys. Rev. B* **2000**, *61*, 10005.
(21) Rijssenbeek, J. T.; Jin, R.; Zadorozhny, Y.; Liu, Y.; Batlogg, B.; Cava, R. J. *Phys. Rev. B* **1999**, *59*, 4561.
(22) Rijssenbeek, J. T.; Matl, P.; Batlogg, B.; Ong, N. P.; Cava, R. J. *Phys. Rev. B* **1998**, *58*, 10315.
(23) Donohue, P. C.; Katz, L.; Ward, W. *Inorg. Chem.* **1965**, *4*, 306.

Table 1. Rietveld Refinement Results for $Ca_3MnRu_2O_9$ and $Ba_3MnRu_2O_9$

	$Ca_3MnRu_2O_9$ (*Pbnm*)	$Ba_3MnRu_2O_9$ ($R\bar{3}m$)
a (Å)	5.347(4)	5.7228(5)
b (Å)	5.463(4)	5.7228(5)
c (Å)	7.610(6)	21.409(7)
V (Å^3)	222.27(2)	607.20(2)
R (%)	5.30	11.15
R_{wp} (%)	10.22	13.78
GOF	1.095	1.179
Bragg *R* (%)	6.27	7.90

Experimental Section

Synthesis. $Ba_3MnRu_2O_9$ and $Ca_3MnRu_2O_9$ were prepared by reacting stoichiometric mixtures of ACO_3 (A = Ba or Ca), RuO_2, and MnO_2 in a platinum crucible at 1100 °C for 24 h, 1200 °C for 48 h, and finally 1260 °C for 48 h (1300 °C for 24 h for the Ca compound) with intermediate grindings. Powder XRD patterns showed that the dark gray polycrystalline products were single phase and free of starting materials.

Characterization. X-ray diffraction data for both samples were collected using a Bruker D8 diffractometer (Cu Kα radiation) at room temperature. Powder diffraction patterns were obtained using a step width of 0.02° at $10° \le 2\theta \le 90°$ in 12 h. Rietveld analysis (Riqas, MDI) was performed to refine the structures of both compounds. Cell refinement calculations were performed on all data and corrected for sample displacements. Profile analysis was conducted using split Pearson VII profile shape functions and procedures previously reported. Initial atomic coordinates and cell constants for $Ca_3MnRu_2O_9$ and $Ba_3MnRu_2O_9$ were taken from the $GdFeO_3$ and $BaRuO_3$ structure types, respectively.[4,23] Various structural models were refined. See text for description.

Magnetic susceptibilities of both compounds were measured with a Quantum Design SQUID magnetometer at an applied field of 100 and 5000 Oe (for Ca and Ba, respectively) in the temperature range 5−300 K. Zero field cooled measurements (ZFC) were performed by cooling the samples to 5 K, applying the field, and measuring the magnetization as the samples were warmed. The field cooled (FC) measurements were done by cooling the sample to 5 K after applying the field and measuring magnetization as the samples were warmed.

Resistance measurements were carried out by using a standard four-probe technique. The compounds were pressed into pellets and annealed at 1050 °C. The calcined cylinders were cut into rectangular blocks, and gold wires were attached to samples with silver paste.

Results

Structures. $Ca_3MnRu_2O_9$ is a prototypical $GdFeO_3$-type perovskite oxide in which the Mn and Ru atoms are randomly distributed over the B sites of the ABO_3 lattice. The structure is orthorhombic, space group *Pbnm*, with typical $GdFeO_3$ lattice parameters (see Table 1). The observed, calculated, and difference XRD patterns obtained from Rietveld analysis are shown in Figure 1. The M−O distances (1.95−1.96 Å) and M−O−M angles (151.2−152.7°) are also typical; the M−O distances are listed in the Supporting Information.

In contrast, $Ba_3MnRu_2O_9$ crystallizes in the 9R rhombohedral structure, space group $R\bar{3}m$, and is isostructural to the 9R polymorph of the $BaRuO_3$ parent compound. In this structure, three MO_6 octahedra share opposite faces to form face-sharing trioctahedra (FSTOs) oriented parallel to the *c* axis of the hexagonal cell. The FSTOs share corners to form a three-dimensional array (see **IV**). Rietveld analyses of the XRD data were carried out by using the atomic coordinates of $BaRuO_3$ as a starting point for the various structural models analyzed.[23] Three different models were considered as possible structures for $Ba_3MnRu_2O_9$. In the first model, Mn and Ru atoms were distributed randomly (33%, 66%) over the two possible B sites

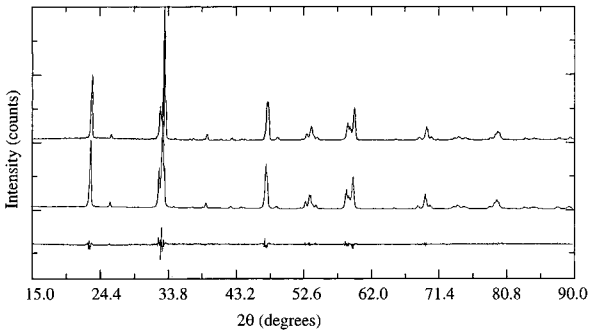

Figure 1. Observed (top), calculated (middle), and difference (bottom) XRD profiles for $Ca_3MnRu_2O_9$.

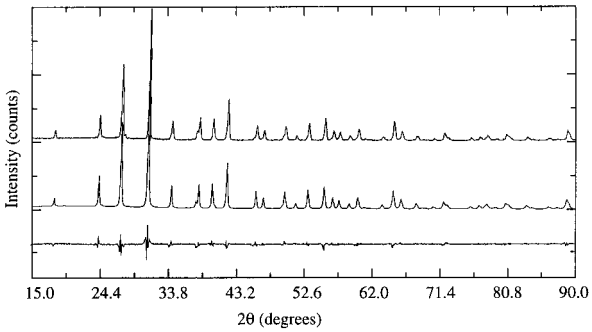

Figure 2. Observed (top), calculated (middle), and difference (bottom) XRD profiles for $Ba_3MnRu_2O_9$.

in the 9R structure. These sites make up the FSTO units and are defined by two terminal octahedra (Wyckoff position 6c) and a middle octahedron (Wyckoff position 3b). In the second model, the Ru and Mn atoms were ordered onto the 6c sites and 3b sites, respectively. The ordered Ru−Mn−Ru trimer model is appealing in that it corresponds to the 2:1 Ru-to-Mn ratio of the compound and is reminiscent of the ordering observed in the related 6H $A_3MRu_2O_9$ compounds reported previously.[22] In a third model, the 6c sites were populated by 50% Ru and 50% Mn and the 3b sites filled exclusively with Ru. Surprisingly, neither of the ordered models gave reasonable refinements whereas the totally disordered model (model 1) gave far superior agreement between calculated and observed XRD profiles. Figure 2 shows the observed, calculated, and difference XRD patterns, and the resulting structural data are listed in Table 1.

The refined FSTO M−M bond distance from the Rietveld analysis was 2.51 Å and is good agreement with the Ru−Ru distance in 9R $BaRuO_3$ (2.55 Å) and related compounds.[24] On the basis of the short M−M separation and the criterion for M−M bonding set forth by Cotton and Ucko,[16] it is clear that there is direct metal−metal bonding in these compounds.

Magnetic and Transport Studies. Figure 3 shows the change in magnetic susceptibility of $Ca_3MnRu_2O_9$ with temperature when recorded in zero field cooled and field cooled conditions. The ZFC susceptibility shows a broad cusp at ~85 K whereas the FC measurements result in a cusp at a lower temperature (70 K). Below 60 K, the FC susceptibility is 1 order of magnitude higher than the ZFC susceptibility. Field dependence of magnetization measured at 5 K shows hysteresis, but saturation is not achieved even at 5 T (Figure 4). The difference in ZFC and FC magnetization is usually indicative of short-range spin-glass- or cluster-glass-like magnetic correlations and

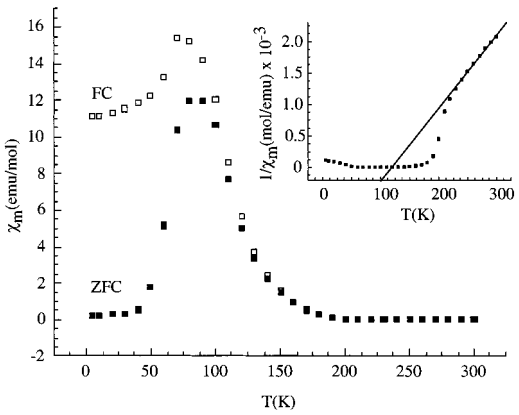

Figure 3. Plot of molar magnetic susceptibility versus temperature for $Ca_3MnRu_2O_9$ recorded at 100 Oe. The inset shows the plot of reciprocal molar susceptibility versus temperature.

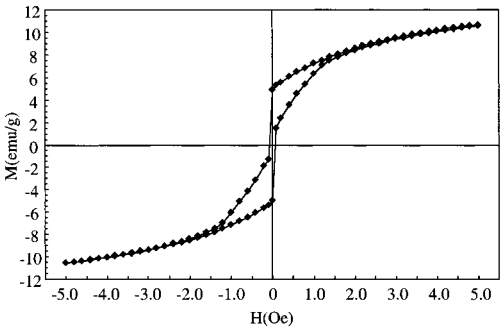

Figure 4. Magnetization versus field plot for $Ca_3MnRu_2O_9$ recorded at 5 K.

signifies the absence of long-range ordering at low temperatures. However, the large magnitude of magnetic susceptibility and the asymptotic approach of high field magnetization value (~10.6 emu/g) to the calculated saturation value for ferrimagnetic ordering (10.7 emu/g) suggests that there is cluster formation in which the magnetic interactions are ferrimagnetic in nature. For comparison, the calculated saturation value for ferromagnetic ordering is 75.1 emu/g. Since there is neither structural ordering (which is necessary for three-dimensional ferrimagnetic ordering) nor saturation in the field dependence of magnetization, we suggest that the compound contains short-range ferrimagnetic interactions without long-range ordering. The positive value of θ (100 K) in the $1/\chi_m$ versus temperature plot (inset of Figure 3) is also consistent with short-range interactions that are ferrimagnetic in nature. Above 240 K, the compound is paramagnetic and follows Curie−Weiss behavior where

$$\chi_m = \frac{C}{T - \theta}$$

The effective magnetic moment is calculated from the equation

$$\chi_m = \frac{N\mu_{eff}^2}{3k(T - \theta)}$$

For $\theta = 100$ K, $\mu_{eff} = 3.14\ \mu_B$ per formula unit of $CaMn_{0.33}Ru_{0.67}O_3$. This value can be used to assign the oxidation states of Mn and Ru in the compound. Three possible oxidation states are Mn(II), 2 × Ru(V); Mn(III), Ru(IV), Ru(V); and Mn(IV), 2 × Ru(IV). It is known that Ru has low-spin orientation in perovskite-related compounds whereas Mn adopts a high-spin

(24) Shepard, M.; McCall, S.; Cao, G.; Crow, J. E. *J. Appl. Phys.* **1997**, *81*, 4978.

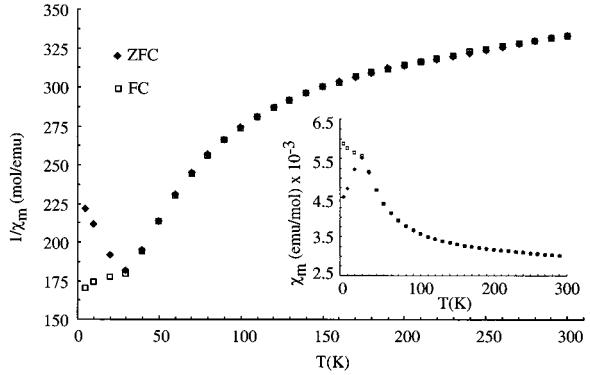

Figure 5. Plot of molar magnetic susceptibility versus temperature for $Ba_3MnRu_2O_9$ recorded at 5000 Oe. The inset shows the plot of reciprocal molar susceptibility versus temperature.

configuration. Since there are two magnetic atoms, the effective magnetic moment can be calculated with the following equation:

$$\mu_{\text{eff}} = \sqrt{\mu_{\text{eff}}{}^2(\text{Ru})(0.6\bar{6}) + \mu_{\text{eff}}{}^2(\text{Mn})(0.3\bar{3})}$$

For the Ru(V)/Mn(II) couple, the calculated spin-only μ_{eff} is 4.6 μ_B; for the Mn(III)/Ru(IV)/Ru(V) system it is 4.2 μ_B; whereas the Mn(IV)/Ru(IV) couple gives a calculated spin-only μ_{eff} of 3.2 μ_B. Our experimental value (3.14 μ_B) is very close to the latter, indicating that Mn and Ru are both in the +4 oxidation state. This finding is also consistent with the fact that Mn and Ru atoms are randomly distributed in the lattice rather than ordered in a double perovskite or other perovskite superstructure. Large differences in the size or charge of B site ions often cause ordering or different crystal structures. The Shannon ionic radii[25] for six-coordinate Mn(IV) and Ru(IV) (low spin) are 0.53 and 0.62 Å, respectively, whereas the radii for Ru(V) and Mn(II) (high spin) are 0.565 and 0.83 Å, respectively.

$Ba_3MnRu_2O_9$ has a low magnetic susceptibility and shows spin-glass-like behavior below 30 K (Figure 5). Although the compound is paramagnetic above 30 K, the data do not obey the Curie−Weiss law for a single-spin system, even with a correction for temperature independent paramagnetism (TIP). Attempted fits of the data to the Curie−Weiss equation give TIPs of 10^{-3} emu/mol and unrealistic Curie constants. We therefore treated the system by way of a variable-spin model in which the effective magnetic moment per formula unit changes with temperature. The effective magnetic moment, μ_{eff}, can be estimated from the Curie−Weiss equation:

$$\chi_m = \frac{Ng^2\mu_B{}^2S(T)(S(T)+1)}{3k(T-\theta)}$$

where $S(T)$ is the spin at temperature T. In our analysis, we assumed a θ value of −30 K on the basis of the location of the cusp in the susceptibility versus temperature plot. The negative value of θ indicates overall antiferromagnetic interactions with short-range competing magnetic correlations below 30 K. The resulting values are not constant (Figure 6) but change with temperature from ∼2.8 μ_B at 300 K to ∼1.7 μ_B at 30 K. These data are inconsistent with a spin-only Mn^{4+} ion (d^3, μ_{eff} ∼ 3.8 μ_B) with only TIP contributions from the Ru^{4+} ions or any other free-ion/TIP combinations. The reduced spin of the $Ba_3MnRu_2O_9$ ground state must therefore result from electron pairing due to direct interatomic interactions and/or strong antiferromagnetic coupling.

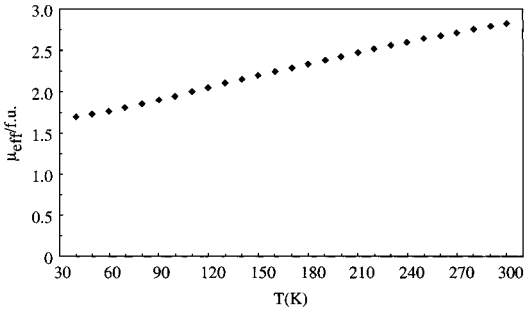

Figure 6. Plot of effective magnetic moment (μ_{eff}) versus temperature. The moments correspond to one formula unit of $Ba_3MnRu_2O_9$.

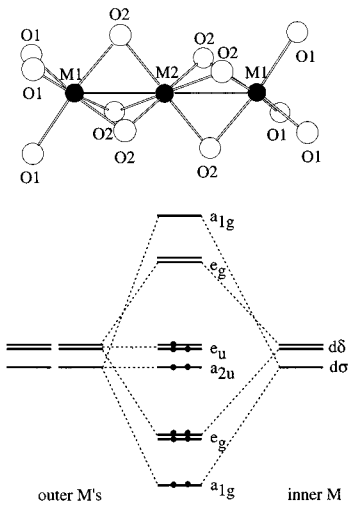

Figure 7. Qualitative molecular orbital diagram for $Ba_3MnRu_2O_9$ showing only the "t_{2g}"-type transition metal d-orbitals. The diagram is modeled directly after that in refs 18 and 19.

If one considers the $MnRu_2O_{12}$ FSTO as a magnetically isolated cluster, the susceptibility of the compound can be modeled with the single spin of the subunit. The FSTO has D_{3h} point symmetry and 11 metal-based electrons (i.e., 2 Ru(IV), d^4, + 1 Mn(IV), d^3). The electronic structures of FSTOs in molecular compounds and extended solids have been described in several reports.[16,19,26] The qualitative MO diagram for the FSTO unit, shown in Figure 7, is analogous to that of $Ru_3Cl_{12}{}^{4-}$ and related compounds.[17−19,27] In all of the analyses, the metal−metal interactions are characterized by a strong σ-bonding component contained in a single, low-lying a_{1g} orbital involving all three metal atoms. At higher energy, there is a block of π/δ-type orbitals along with an additional σ-nonbonding orbital, the a_{2u}. Depending on the M−M separation, these π/δ-type interactions are quite weak and can be considered essentially nonbonding. The short M−M separation (2.51 Å) and the relatively acute O2−M2−O2 angle (78°) in the present compound indicate that direct M−M bonding is present.[16] For comparison, the Ru−Ru separation in the Ru(II)−Ru(III)−Ru(III) FSTO $Ru_3Cl_{12}{}^{4-}$ is 2.80 Å where strong metal−metal bonding has been established.[18,19] On the basis of comparisons with other odd-electron FSTO compounds,[17] one would expect an $S = {}^1/_2$ $(a_{1g})^2(e_g)^4(a_{2u})^2(e_u)^3$ ground state system with thermally populated higher spin states providing a significant contribution at higher

(25) Shannon, R. D. *Acta Crystallogr.* **1976**, *A32*, 751.

(26) Chen, B.-H.; Eichhorn, B. W.; Ju, H. L.; Greene, R. L. *Inorg. Chem.* **1993**, *32*, 5715.

(27) Fettinger, J. C.; Mattamana, S. P.; O'Connor, C. J.; Poli, R. *J. Chem. Soc., Chem. Commun.* **1995**, 1265.

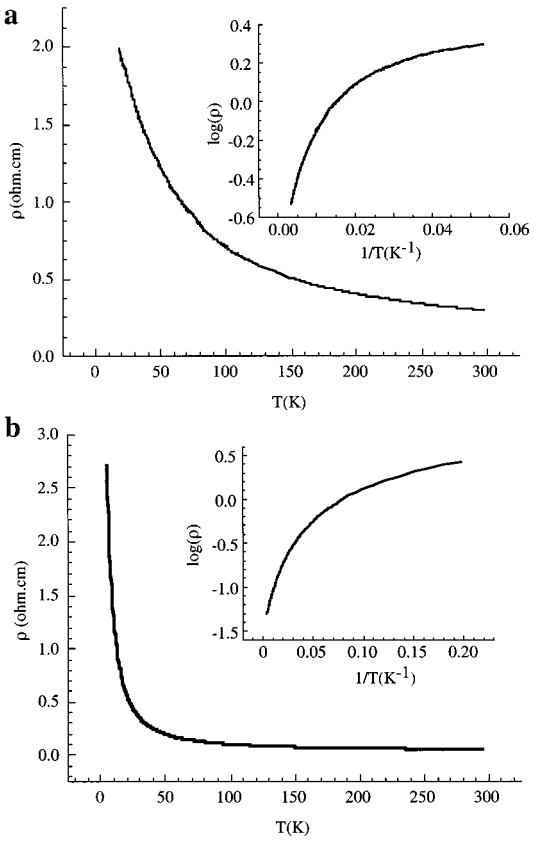

Figure 8. (a) Plot of resistivity versus temperature for $Ca_3MnRu_2O_9$. (b) Plot of resistivity versus temperature for $Ba_3MnRu_2O_9$. The insets show respective plots of log resistivity versus inverse temperature.

temperatures. The extracted moments shown in Figure 6 are in excellent agreement with an $S = {}^1/_2$ ground state (expected $\mu_{\text{eff}} \sim 1.7\ \mu_B$).

Panels a and b of Figure 8 show the resistivity versus temperature plots for $Ca_3MnRu_2O_9$ and $Ba_3MnRu_2O_9$, respectively. Both compounds are semiconductors with low room-temperature resistivities of ca. 58 and 5.1 mΩ·cm, respectively. The plots of log ρ versus inverse temperature (Figure 8 insets) are linear above 200 K but nonlinear at lower temperatures. The activation energies can be calculated from the linear regions by using the equation

$$\rho = \rho_0 e^{E_a/kT}$$

where the slope of the log ρ vs $1/T$ plot is

$$\text{slope} = \frac{E_a}{2.303k}$$

The calculated activation energies are 17 and 8.8 meV for $Ca_3MnRu_2O_9$ and $Ba_3MnRu_2O_9$, respectively. Attempts to fit the low-temperature data to different variable-range hopping models did not give satisfactory results. It is possible that the carrier concentrations are changing at low temperatures or that impurities dominate the transport in this region.

Discussion

In a previous study, we examined the magnetic properties of $BaVO_{2.8}$, which adopts the 9-layer 9R structure, with a two-term susceptibility model.[26] The $V_3O_{12}^{12-}$ unit (a FSTO) was treated as an isolated spin center where 2 of the metal-based electrons were paired in a metal−metal σ-bond. In $Ba_3MnRu_2O_9$, the $S = {}^1/_2$ ground state requires 10 of the 11 metal-based electrons to be paired in the a_{1g} σ-orbital, 2 of the π/δ-type orbitals, and the a_{2u} nonbonding orbital (see Figure 7). The situation is directly analogous to the 9-electron $Mo_3X_{12}^{3-}$ molecular complexes (X = halide) which also have $S = {}^1/_2$ ground states.[9,17] The *relatively* large energy difference between the e_u and e_g orbitals is consistent with the short Ru−Ru separations and the $S = {}^1/_2$ ground state of the compound.

In contrast, the Mn(IV) and Ru(IV) ions in the isoelectronic $Ca_3MnRu_2O_9$ phase ($GdFeO_3$ structure) show spin-only moments for both ions. The related 6H $Ba_3MRu_2O_9$ phases in which the Ru and M atoms are *completely* ordered in the face- and corner-shared octahedra, respectively, show spin-only moments for the M ions and temperature independent paramagnetism for the Ru_2O_9 FSBO units.[22] Again, the Ru moments are suppressed due to strong metal−metal bonding. Interestingly, only the Fe phase shows a suppressed moment that has been attributed to the disordering of Fe and Ru between the FSBO and the corner-shared perovskite layer of the 6H structure.[22] Incorporation of the Fe^{3+} ion in the FSBO apparently forces pairing of electrons in the form of metal−metal bonds which yields lower spin values than those expected from spin-only high-spin complexes.

Finally, it is interesting to note that only the Mn member of the $Ba_3MRu_2O_9$ phases adopts the disordered 9R structure whereas the remainder of the $Ba_3MRu_2O_9$ phases (where M = Fe, Co, Ni, Cu, In) form ordered (or partially ordered) 6H structures. In addition, the $GdFeO_3$ perovskite phase $Ca_3MnRu_2O_9$ shows complete disordering of the Mn and Ru ions. We propose that the disorder in the two structures is due not only to the similarities in size but also to the ability of Mn to undergo valence fluctuation. This process not only enhances disorder but also gives rise to nearly metallic conductivity in both phases. The room-temperature resistivity of $Ba_3MnRu_2O_9$ is substantially lower than the room-temperature resistivities of the other $Ba_3MRu_2O_9$ phases and illustrates the effects of valence degeneracy between Mn(IV) and Ru(IV) and atomic ordering.

Supporting Information Available: M−O (M = Mn, Ru) and O−O distances of $Ca_3MnRu_2O_9$. This material is available free of charge via the Internet at http://pubs.acs.org.

Acknowledgment. We gratefully acknowledge the NSF (DMR-0076460) for support of this research and Dr. Vera Smolyaninova for helpful discussions.

IC0013431